# Evolution of the resistivity anisotropy in $Bi_2Sr_{2-x}La_xCuO_{6+\delta}$ single crystals for a wide range of hole doping

S. Ono and Yoichi Ando[*]

*Central Research Institute of Electric Power Industry, Komae, Tokyo 201-8511, Japan*

(Dated: February 1, 2008)

To elucidate how the temperature dependence of the resistivity anisotropy of the cuprate super-conductors changes with hole doping, both the in-plane and the out-of-plane resistivities ($\rho_{ab}$ and $\rho_c$) are measured in a series of high-quality $Bi_2Sr_{2-x}La_xCuO_{6+\delta}$ (BSLCO) single crystals for a wide range of $x$ ($0.23 \leq x \leq 1.02$), which corresponds to the hole doping per Cu, $p$, of 0.03 – 0.18. The anisotropy ratio, $\rho_c/\rho_{ab}$, shows a systematic increase with decreasing $p$ at moderate temperatures, except for the most underdoped composition where the localization effect enhances $\rho_{ab}$ and thus lowers $\rho_c/\rho_{ab}$. The exact $p$ dependence of $\rho_c/\rho_{ab}$ at a fixed temperature is found to be quite peculiar, which is discussed to be due to the effect of the pseudogap that causes $\rho_c/\rho_{ab}$ to be increasingly more enhanced as $p$ is reduced. The pseudogap also causes a rapid growth of $\rho_c/\rho_{ab}$ with decreasing temperature, and, as a result, the $\rho_c/\rho_{ab}$ value almost reaches $10^6$ in underdoped samples just above $T_c$. Furthermore, it is found that the temperature dependence of $\rho_c$ of underdoped samples show two distinct temperature regions in the pseudogap phase, which suggests that the divergence of $\rho_c$ below the pseudogap temperature is governed by two different mechanisms.

## I. INTRODUCTION

It has long been recognized that the peculiar $c$-axis transport properties[1] of the high-$T_c$ cuprates are strong manifestations of the unusual electronic state in these materials.[2] In particular, the following two features have been considered to be most unusual: (i) The magnitude of the $c$-axis resistivity $\rho_c$ is orders of magnitude larger than that expected from band calculations,[3] leading to a huge resistivity anisotropy where $\rho_c$ is up to $10^5$ times larger[4] than the in-plane resistivity $\rho_{ab}$. (ii) The temperature dependence of $\rho_c$ is in most cases semiconducting or insulating (i.e., $d\rho_c/dT < 0$), while that of $\rho_{ab}$ is metallic ($d\rho_{ab}/dT > 0$); such a contrasting behavior[5,6,7] is not expected in ordinary anisotropic metal.[1,2]

The feature (i) indicates that the strong correlations in the cuprate materials give rise to some unconventional mechanism which renormalizes the $c$-axis transfer-matrix element to a value much smaller than what is expected for an uncorrelated system. This renormalization of the $c$-axis transfer-matrix element is usually called "charge confinement". There have been many theoretical proposals to explain the charge confinement in the cuprates, but it is fair to say that the confinement mechanism is not yet understood on the fundamental level. Since many of the theoretical models for the charge confinement, such as the resonating-valence-bond theories[8,9] or self-organized stripe theories,[10,11] are closely tied to the mechanism of the high-$T_c$ superconductivity, it remains to be important to study the $c$-axis transport in the cuprates.

The feature (ii) is now better understood than the feature (i), both experimentally and theoretically, though the understanding is still far from complete. To appreciate the current understanding of the feature (ii), it should first be recognized[12] that the $c$-axis transport in the normal-state of the cuprates is essentially an incoher-ent tunneling process; this fact gives rise to the intrinsic Josephson effect[13] as well as the Josephson-plasma resonance[14] in the superconducting state. It should at the same time be noted that the tunneling conductance for ordinary metal-insulator-metal junctions should be *independent* of temperature, according to the Fermi golden rule; this means that the "semiconducting" behavior of $\rho_c(T)$ does *not* automatically arise from the tunneling nature of the $c$-axis transport. (In this sense, the expression "semiconducting behavior", which implies that the transport is essentially an activation process over a gap, is inappropriate, though this expression is often naively used in this context.) Thus, there must be some unconventional mechanisms which cause the peculiar "insulating" temperature dependence of $\rho_c$ in the cuprates.

Experimentally, there seem to be two additive mechanisms that are both responsible for the "insulating" $\rho_c(T)$. The first is the charge-confinement mechanism which appears to become increasingly more effective with lowering temperature; this causes the tunneling matrix element to be reduced and keeps $\rho_c$ increasing with decreasing $T$. This point was most clearly demonstrated[7] by the low-temperature normal-state resistivity measurement of $Bi_2Sr_{2-x}La_xCuO_{6+\delta}$ (BSLCO) under 60 T, which showed that $\rho_c$ of Bi-2201 keeps increasing even down to 0.6 K. The more recently recognized mechanism is the effect of the pseudogap[15] which causes destruction of the Fermi surface starting from the $(\pm\pi, 0)$, $(0, \pm\pi)$ points, as has been demonstrated by angle-resolved photoemission spectroscopy (ARPES) measurements[16]; this causes the available density of states (DOS) for tunneling to be reduced, and $\rho_c$ gets steeply increased as the pseudogap develops. Note that the $c$-axis matrix element of the cuprates has a particular $\mathbf{k}$-dependence[17] ($\mathbf{k}$ is the in-plane wave vector of the conduction electrons) that tends to amplify the contribution of the elec-

trons on these gapped portion of the Fermi surface, and this **k**-dependence of the matrix element causes $\rho_c$ to be very sensitive to the opening of the pseudogap.[12] Recent tunneling-spectroscopic studies[18,19] of the intrinsic junctions in $Bi_2Sr_2CaCu_2O_{8+\delta}$ (Bi-2212) have made strong cases for the interpretation that the steep upturn in $\rho_c(T)$ below the pseudogap temperature $T^*$ is largely due to this second mechanism. It is expected that these two independent mechanisms, confinement and pseudogap, together cause the rather complicated, "insulating" $\rho_c(T)$ behavior in the cuprates, though their relative roles in determining the actual temperature dependence is not clarified yet.

Given the above-mentioned recent understanding of the $c$-axis transport, it would be instructive to see how the two mechanisms (confinement and pseudogap) are actually working in a single system. For such a purpose, it is useful to elucidate the evolution of the behavior of $\rho_c(T)$, as well as the anisotropy ratio $\rho_c/\rho_{ab}$, over a wide range of hole doping, because $T^*$ is known to decreases with increasing doping. In the past, there were many studies of the anisotropic resistivities in $La_{2-x}Sr_xCuO_4$ (LSCO),[5,20,21,22] $YBa_2Cu_3O_{7-\delta}$ (YBCO),[6,23] Bi-2212,[24] and BSLCO,[4,25] but none of them cover a wide enough doping range from underdoped insulators to overdoped superconductors to yield a coherent picture.

Very recently, Komiya *et al.* measured[26] the anisotropic resistivity of high-quality LSCO single crystals for $x = 0.01 - 0.10$ and found that in this system the effect of pseudogap is *not* apparent (i.e., the additional mechanism to cause the insulating $\rho_c(T)$ is absent), probably because of the unique Fermi surface topology[27,28] of LSCO. Therefore, it is useful to study another cuprate system in which one can change the hole doping over a really wide range. Obviously, BSLCO is an ideal candidate, because we have demonstrated[29,30,31] that the hole doping can be varied (by changing the La concentration) from heavily-underdoped insulator to overdoped superconductor; moreover, ARPES measurements have found[32,33,34] that the Fermi surface topology and the pseudogap structure of BSLCO are very similar to those of Bi-2212. We can thus expect that it may be possible to substantiate the effects of charge confinement and the pseudogap on the $c$-axis transport by tracing its evolution with the hole doping in BSLCO.

The purpose of this paper is to provide high-quality data, obtained from well-controlled experiments, on the evolution of the temperature dependences of $\rho_c$ and $\rho_c/\rho_{ab}$ of BSLCO for a wide range of doping, which showcases the complicated origin of the unusual $c$-axis transport in the cuprates. Our data exemplifies that there are three different mechanisms that govern the behavior of the anisotropy ratio $\rho_c/\rho_{ab}$: charge confinement, pseudogap, and localization. In particular, the temperature dependence of $\rho_c$ of our underdoped samples makes a good case for the two different origins of the insulating behavior below $T^*$.

This paper is organized as follows: Details of our crystal-growth technique to produce the high-quality BSLCO single crystals, as well as the details of our measurement technique, are presented in Section II. Section III presents our data for $\rho_{ab}(T)$, $\rho_c(T)$, and $\rho_c/\rho_{ab}$, putting emphasis on how they evolve with changing hole doping. The implication of the systematics of our observation is discussed in Section IV, and Section V summarizes our findings.

## II. EXPERIMENTS

### A. $Bi_2Sr_{2-x}La_xCuO_{6+\delta}$ Crystals

The $Bi_2Sr_{2-x}La_xCuO_{6+\delta}$ system is a Bi-based single-layer cuprate where the hole doping is controlled by replacing Sr with La. Until a few years ago, this material had been considered to be a particularly "dirty" system among the cuprates, because the in-plane resistivity of even the best crystal at those times showed the residual resistivities of around 70 $\mu\Omega$cm (Refs. 4,7) and the Hall coefficient $R_H$ displayed only a weak temperature dependence,[35] both of which are characteristic of dirty cuprate samples.

In 1999, Ando and Murayama demonstrated[29] that it is possible to grow high-quality single crystals of BSLCO that show much smaller residual resistivity and a strongly temperature-dependent $R_H$, which conform to the "standard" behavior of cuprates. Also, though the BSLCO system was believed to possess the lowest optimum $T_c$ among the well-studied cuprate systems, we have demonstrated[30] that the optimum $T_c$ of this system can be raised to 38 K, which is almost equal to the optimum $T_c$ of LSCO.

In BSLCO, larger La concentration $x$ corresponds to smaller hole doping per Cu, $p$, and the relation between $x$ and $p$, as well as the phase diagram of $T_c$ vs $p$, has been sorted out[31]; it was found that optimum doping occurs at $p \simeq 0.16$ (which is achieved with $x \simeq 0.4$), but the superconductivity disappears at $p \simeq 0.10$ ($x \simeq 0.8$) upon underdoping. Low-temperature normal-state resistivity measurement of this system using 60-T pulsed magnetic field found[30] that the metal-to-insulator crossover occurs at $p \simeq 1/8$, below which $\rho_{ab}(T)$ shows a peculiar $\log(1/T)$ divergence.

Single crystals of $Bi_2Sr_{2-x}La_xCuO_{6+\delta}$ are grown by the floating-zone (FZ) technique for a wide range of La concentration ($0.23 \leq x \leq 1.02$). Before the FZ operation, we first prepare polycrystalline rods of BSLCO. Raw powders of $Bi_2O_3$, $SrCO_3$, $La_2O_3$, and CuO, with purities of 99.9% or higher, are dried, weighed, mixed into the nominal molar ratio of the target composition, and well ground in an agate mortar; they are then calcined at $750 - 850°C$ for 20 hours to form the BSLCO phase. The resulting powders are reground and calcined again, and this process is repeated twice. The x-ray diffraction analysis reveals that the powders become 100%-pure BSLCO phase after the third calcination. The resulting BSLCO

TABLE I: Actual composition of the obtained crystals for each nominal (starting) La concentration. The molar ratios of the cations are determined by ICP-AES and are shown with the Cu value fixed to 1.

| nominal La composition | Bi | Sr | La | Cu |
|---|---|---|---|---|
| 0.20 | 2.02 | 1.70 | 0.23 | 1 |
| 0.40 | 1.98 | 1.59 | 0.39 | 1 |
| 0.50 | 1.99 | 1.52 | 0.49 | 1 |
| 0.60 | 1.93 | 1.31 | 0.66 | 1 |
| 0.70 | 2.00 | 1.30 | 0.73 | 1 |
| 0.80 | 2.00 | 1.17 | 0.84 | 1 |
| 0.90 | 1.92 | 1.06 | 0.92 | 1 |
| 1.00 | 1.90 | 0.98 | 1.02 | 1 |

TABLE II: Actual hole concentrations per Cu, $p$, and $T_c$ for each La concentration $x$. The $p$ values are determined from the empirical relation between $x$ and $p$ obtained in Ref. 31.

| $x$ | 0.23 | 0.39 | 0.49 | 0.66 | 0.73 | 0.84 | 0.92 | 1.02 |
|---|---|---|---|---|---|---|---|---|
| $p$ | 0.18 | 0.16 | 0.14 | 0.12 | 0.11 | 0.10 | 0.07 | 0.03 |
| $T_c$ | 29 | 38 | 31 | 23 | 14 | 1.4 | 0 | 0 |

powders are isostatically pressed into a rod shape ($\approx 5$ mm$\phi$ × 100 mm) and finally sintered at 850°C for 20 hours, to form a rigid polycrystalline feed rod to be used for the FZ operation.

Single-crystal growth is carried out using an infrared image furnace (NEC Machinery SC K-15HD) with two halogen lamps and double ellipsoidal mirrors. We grow BSLCO crystals with a "simple" FZ technique, which means that we do not use any solvent to reduce the temperature of the molten zone. One important technique we use is what we call "fast scan", with which we quickly melt and quench the whole feed rod using the FZ furnace with the feed speed of 30 mm/h. This process is necessary for making the feed rod dense, which is important for avoiding the emergence of bubbles during the crystal growth; actually, the rod becomes appreciably thinner than the as-sintered rod after the fast scan (it becomes roughly 3 mm$\phi$). The "scanned" rod is then remounted to the FZ furnace and is used for the actual crystal growth. The growth rate is kept constant at 0.5 mm/h, which is two times slower than the growth rate for LSCO.[26] Another important technique we use during the growth is what we call "necking"; since many independent domains start to crystallize at the initial stage of the growth, after roughly 1 cm of the rod is grown, the diameter of the molten zone is gradually reduced to approximately 2 mm$\phi$, which causes fewer domains to remain in the crystal. The molten zone is then gradually fattened, which leads to the growth of the fewer domains in the resulting rod. After a few times of the necking, when the growth is successful, there remains only one domain and the whole chunk becomes a large single-domain crystal. The space around the molten zone is filled with 1 atm of flowing oxygen during the growth of underdoped crystals, while for the growth of overdoped crystals the space is filled with 1 atm of flowing air. The size of the single-domain crystals that can be obtained from the grown rod is typically 20 × 3 mm$^2$.

The actual La concentrations in the crystals are determined by the inductively-coupled plasma atomic-emission spectroscopy (ICP-AES). The crystals tend to contain more La than the nominal composition, but the difference is small; here we report crystals with actual $x$

values of 0.23, 0.39, 0.49, 0.66, 0.73, 0.84, 0.92, and 1.02, and these crystals were obtained from the nominal $x$ values of 0.20, 0.40, 0.50, 0.60, 0.70, 0.80, 0.90, and 1.00, respectively. In all these crystals, the ICP-AES analysis confirms that there is essentially no excess Bi in the crystals; rather, Bi tends to be deficient in highly La-doped crystals, as shown in Table I. On the other hand, the ratio of (Sr+La):Cu is always near 2:1.

Uniformity of the distribution of the La dopants in the crystals is confirmed by the electron-probe microanalysis (EPMA), with which the variation of the $x$ value is estimated to be within 5%. The superconducting transition temperature $T_c$ is determined both by the zero resistivity in the transport measurement and by the onset of the Meissner signal in the SQUID magnetization measurement; for all the crystals reported here, these two definitions give $T_c$ values that match within ±0.5 K, and the variation among different pieces of crystals with the same composition is also within ±0.5 K. (Thus we refer to the $T_c$ values with two significant digits in this paper.) The $T_c$ values for each of the compositions are listed in Table II.

### B. Measurements

The crystals are cut into dimensions of typically 2 × 1 × 0.05 mm$^3$ for the $\rho_{ab}$ measurements and 1 × 1 × 0.05 mm$^3$ for the $\rho_c$ measurements. Accurate determination of the crystal thickness is done by measuring the weight with 0.1 $\mu$g resolution and converting it into volume using the nominal density for each composition. We employ the straightforward four-terminal method to measure $\rho_{ab}$ and $\rho_c$: For the $\rho_{ab}$ measurements, the current contacts are painted to cover two opposing side faces of the platelet-shaped crystals to ensure a uniform current flow and the voltage contacts are painted on the two remaining side faces of the crystals. For the $\rho_c$ measurements, two current contacts are painted to almost completely cover the opposing $ab$ faces of the crystal and two voltage contacts are placed in the small window reserved in the center of the current contacts. In both cases, the contact pads are tactfully hand-drawn with gold paint, followed by a heat treatment at 400°C for 30 minutes in the air, which makes the gold particles to well adhere to the sample surface. After this heat-treatment to cure the gold contact pads, the samples are annealed at higher temperatures for longer time to control the oxygen concentration; samples with $x$ larger than 0.3 are annealed
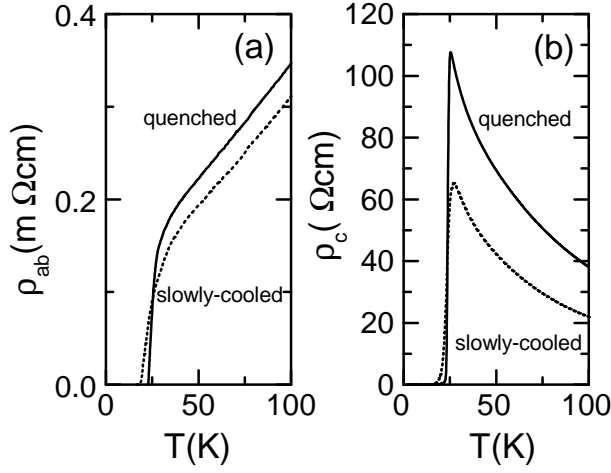
FIG. 1: Temperature dependences of (a) $\rho_{ab}$ and (b) $\rho_c$ of the BSLCO crystals with $x = 0.66$ ($p = 0.12$); quenched samples (solid lines) and slowly-cooled samples (dotted lines) show non-negligible difference, even though the annealing conditions are the same.



FIG. 2: (a) Temperature dependences of $\rho_{ab}$ of the BSLCO crystals for various $p$. (b) Semi-logarithmic plot of $\rho_{ab}$(T).

in flowing air at 650°C for 48 hours, while those with $x \leq 0.3$ are annealed in flowing oxygen at 400°C for 60 hours. In both cases, the crystals are annealed together with a sufficient amount of BSLCO powders of the same composition, and they are quenched to room temperature at the end of the annealing. Finally, gold lead wires are attached to the contact pads using silver epoxy, which is cured at relatively low temperature, 130°C. The contact resistance we achieve with this technique is less than 1 Ω. We note that the above annealing conditions are chosen to minimize the superconducting transition width $\Delta T_c$ of our crystals; in all the superconducting samples, $\Delta T_c$ in $\rho_c(T)$ data is around 2 K after the above annealing.

Before finishing the description of our sample preparation technique, we would like to emphasize the importance of the quenching at the end of the high-temperature annealing. Figure 1 shows the data of $\rho_{ab}(T)$ and $\rho_c(T)$ of our BSLCO crystals with $x = 0.66$, for both quenched and slowly-cooled samples. Although both sets of the samples are annealed at 650°C for 48 hours, the data show non-negligible differences; the difference in the $\rho_{ab}(T)$ are comparatively small (the magnitude of $\rho_{ab}$ of quenched sample is 10% larger than that of slowly-cooled sample), but the difference in $\rho_c(T)$ is significant, differing by about 50%. Also, $\Delta T_c$ is about 2 K for the quenched samples, while it is about 6 K for the slowly-cooled sample. Those differences are consistent with the interpretation that the slow cooling causes the oxygen concentration in the samples to be inhomogeneous and there are more oxygen near the surface of the slowly-cooled samples; remember that the equilibrium oxygen concentration of Bi-2201 during the annealing is dependent on both the temperature and the oxygen partial pressure, and the equilibrium concentration becomes higher as the temperature is lowered. Thus, to
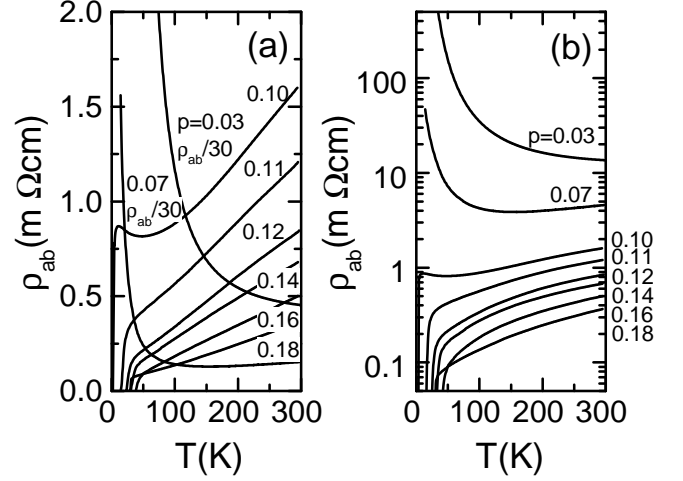
obtain uniformly oxygenated samples and reproducible data, quenching is indispensable.

In this work, we measure $\rho_{ab}$ and $\rho_c$ on more than 20 samples for each La concentration to check for the reproducibility; the variation in the absolute magnitude of the resistivity of the quenched sample is less than ±10%, which is consistent with the size of the errors due to uncertainties in the geometrical factors.

We have previously determined the actual hole concentration per Cu, $p$, for various La concentrations $x$, and have obtained an empirical relation.[31] In this paper we use this empirical relation to convert $x$ into $p$, which are listed in Table I. Hereafter we mostly use the $p$ value in referring to the samples, because $p$ is much more intuitively understandable than $x$.

### III. RESULTS

#### A. In-plane resistivity

Figure 2 shows the temperature dependences of $\rho_{ab}$ for all the $p$ values studied here. As expected (and has been reported in Refs. 29,30,31), the magnitude of $\rho_{ab}(T)$ shows a systematic increase with decreasing carrier concentration from $p = 0.18$ to 0.03. The $\rho_{ab}(T)$ curve of the overdoped sample ($p = 0.18$) shows a behavior that can be described[29] by $a + bT^n$ with $n > 1$, while a strictly $T$-linear behavior is apparent in the optimally-doped sample ($p = 0.16$). In the most underdoped non-superconducting sample ($p = 0.03$), $\rho_{ab}(T)$ shows an insulating behavior ($d\rho_{ab}/dT < 0$) from room temperature, which is quite different from the $\rho_{ab}(T)$ behavior of lightly hole-doped LSCO that shows a metallic behavior ($d\rho_{ab}/dT > 0$) even at $x = 0.01$.[36] We assert this difference is not intrinsic but is rather due to disorder, because the room-temperature sheet resistance per CuO$_2$ plane of

our BSLCO at $p = 0.03$ is 110 k$\Omega$, while that of LSCO at $x = 0.03$ (Ref. 36) is only 60 k$\Omega$; this indicates that a significant disorder is present in the heavily-underdoped BSLCO samples. On the other hand, the residual resistivity at optimum-doping ($p = 0.16$) is only 20 $\mu\Omega$cm, indicating that the electron transport can be quite clean in this system; since we find that the crystals are morphologically very clean for both $p = 0.03$ and 0.16, the source of the electronic disorder is apparently not any crystalline defects but is likely to be the local disordering potentials due to the La dopants.

It is useful to note that the barely superconducting sample, $p = 0.10$, shows $\rho_{ab}$ value of $\sim 0.7$ m$\Omega$cm just above $T_c$; this value corresponds to the sheet resistance per CuO$_2$ plane of 5.8 k$\Omega$, which is very close to the quantum sheet resistance $h/4e^2$ ($= 6.45$ k$\Omega$). This suggests that the disappearance of the superconductivity in BSLCO at unusually high doping of $p \simeq 0.10$ is caused by the disorder-driven superconductor-insulator transition in two-dimensional (2D) superconductors.[37]

## B. Out-of-plane resistivity

Figure 3 shows the temperature dependences of $\rho_c$ for the same compositions as those in Fig. 2. As is the case with $\rho_{ab}(T)$, the magnitude of $\rho_c(T)$ shows a systematic increase with decreasing carrier concentration. Since the magnitude of $\rho_c$ changes by 2 orders of magnitude from $p = 0.18$ to 0.03, the data for the overdoped and optimally-doped samples are shown in Fig. 3(a), while those of the underdoped samples are shown in Fig. 3(b), both in linear scale; Fig. 3(c) plots $\rho_c(T)$ in semi-logarithmic scale to equally show the behavior of all the samples. In Fig. 3(a), $\rho_c(T)$ data for La-free Bi$_{2.13}$Sr$_{1.89}$CuO$_{6+\delta}$ ("pure" sample) are also shown for comparison (dotted line). It is worthwhile to note that, for each composition, the $\rho_c$ value of our crystals is generally smaller than that reported for BSLCO in the past.[4,25]

We note that a "metallic" temperature dependence of $\rho_c$ is often observed, as is the case with the present experiment, in overdoped samples at high enough temperatures,[5,6,38,39] which probably indicates that the in-plane scattering of the electrons is involved in determining the temperature dependence of $\rho_c$.[40] In fact, recent $c$-axis magnetoresistance study by Hussey *et al.* showed that $\rho_c$ of LSCO is strongly affected by the scattering within the planes.[41] This suggests that looking at $\rho_c/\rho_{ab}$ is useful for investigating the intrinsic mechanisms of the unusual $c$-axis transport, because the in-plane scattering rate is roughly cancelled out in $\rho_c/\rho_{ab}$.

## C. Anisotropy ratio $\rho_c/\rho_{ab}$

Figure 4 shows the temperature dependences of the anisotropy ratio $\rho_c/\rho_{ab}$ for all the concentrations studied. At moderate temperatures, the magnitude of $\rho_c/\rho_{ab}$

monotonically increases with decreasing $p$, except for the most underdoped concentration ($p = 0.03$) at which $\rho_c/\rho_{ab}$ suddenly drops; it is probably the case that this drop is caused by the heightened $\rho_{ab}$ value of the $p = 0.03$ sample due to localization, and therefore if there were no enhanced disorder at this composition we would expect $\rho_c/\rho_{ab}$ to be not much different from that for $p = 0.07$. Note that the $\rho_c/\rho_{ab}$ value generally increases with lowering temperature, and almost reaches $10^6$ just above $T_c$ for $p = 0.10 - 0.14$.

Before our FZ-grown crystals became available, the anisotropic resistivity of BSLCO was measured by Wang *et al.* using flux-grown crystals that showed rather large residual resistivities.[25] Though the data by Wang *et al.* demonstrated reasonably systematic behavior and are mostly consistent with our data reported here, their data are different from ours in one important aspect: they observed that the anisotropy ratio $\rho_c/\rho_{ab}$ is almost independent of doping at 300 K, while we observed that $\rho_c/\rho_{ab}$ at 300 K increases systematically with decreasing $p$, as can be seen in Fig. 4.

We note that in the anisotropic resistivity measurements using the flux-grown crystals, it was already recognized that the BSLCO system shows a very large anisotropy ratio $\rho_c/\rho_{ab}$ of more than $10^5$, which is the largest among the cuprates; for example, Martin *et al.* reported[4] that $\rho_c/\rho_{ab}$ can be as large as $3 \times 10^5$ in Bi-2201, and the work by Wang *et al.* mentioned above reported[25] maximum $\rho_c/\rho_{ab}$ of $2.5 \times 10^5$. In our crystals, perhaps because of the smaller $\rho_{ab}$ values, the observed $\rho_c/\rho_{ab}$ is even larger: the $\rho_c/\rho_{ab}$ value exceeds $5 \times 10^5$ in four of the concentrations ($p = 0.10$, 0.11, 0.12, and 0.14), and the maximum $\rho_c/\rho_{ab}$ we observe is $8 \times 10^5$.

## IV. DISCUSSIONS

### A. La-free ("pure") sample

In Fig. 3, one can infer that the onset of steeply insulating behavior in $\rho_c(T)$ moves to higher temperature with decreasing $p$ in the La-doped series of samples, which is consistent with the expected behavior of the pseudogap-opening temperature $T^*$. Although the data for pure sample in Fig. 3(a) appears to conform nicely to this trend, there is one issue that we need to elaborated on: When we estimate the actual hole concentration of the pure sample using the method we reported in Ref. 31, the $p$ value of this pure sample is 0.17 [Fig. 5(a)]; the slope of $\rho_{ab}(T)$ also indicate that the $p$ value of the pure samples should be around 0.17 [Fig. 5(b)]. On the other hand, compared to the La-doped $p = 0.18$ sample, the $\rho_c$ value of the pure sample is *smaller* and the onset temperature of the insulating behavior is *lower*, both of which would normally be expected for more *overdoped* sample. Although this apparent puzzle looks problematic, it can be understood to be a result of a combination of extrinsic effects: First, since the constituent
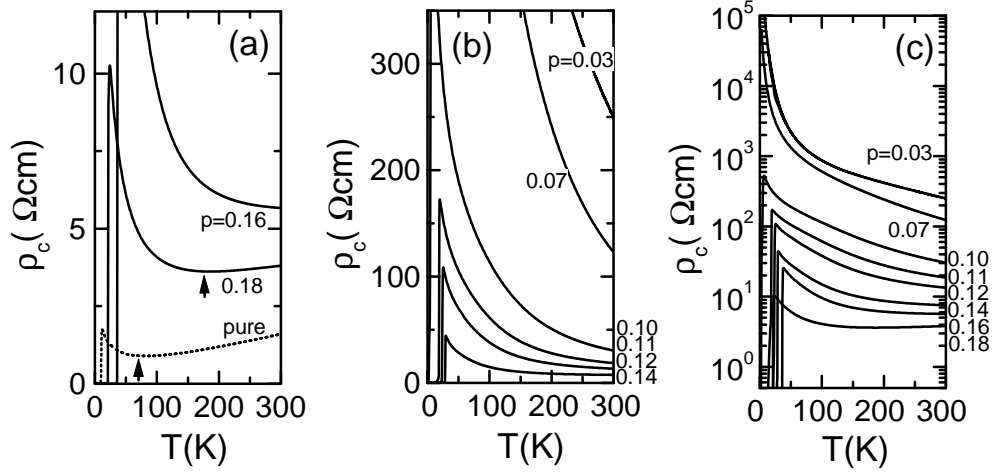
FIG. 3: Temperature dependences of $\rho_c$ of the BSLCO crystals for (a) $0.16 \leq p \leq 0.18$ and (b) $0.03 \leq p \leq 0.14$. Panel (a) also includes $\rho_c(T)$ data of "pure" sample (La-free $Bi_{2.13}Sr_{1.89}CuO_{6+\delta}$). Arrows mark the temperature where $\rho_c(T)$ shows a minimum. (c) Semi-logarithmic plot of $\rho_c(T)$ for all the $p$ values.
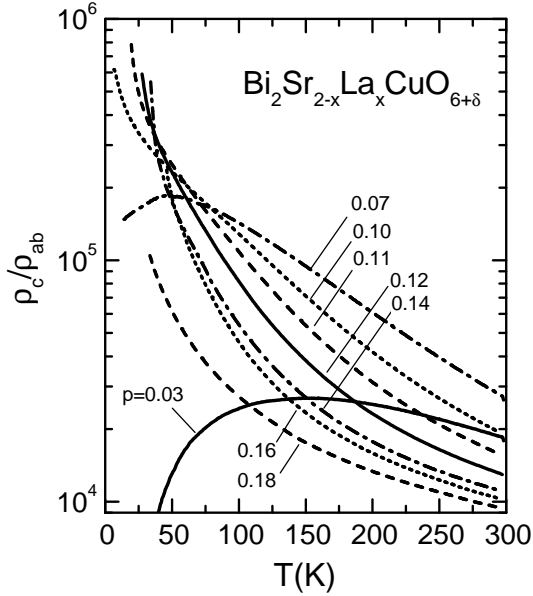


FIG. 4: Temperature dependences of $\rho_c/\rho_{ab}$ of the BSLCO crystals calculated from the data in Figs. 2 and 3.



FIG. 5: (a) Plots of the renormalized Hall coefficient, $R_H e/V_0$, vs $T$ for the pure sample and the BSCLO samples with $p = 0.16$ and $0.18$, where $V_0$ is the volume per one Cu atom in the unit cell; the values of $R_H e/V_0$ of various cuprates near room temperature have been found to agree for the same $p$ value, giving a good tool to estimate $p$.[31] (b) Comparison of the $\rho_{ab}(T)$ data of the pure sample to those of BSLCO with $p = 0.16$ and $0.18$.

atoms of the apical-oxygen layer are different [(Sr,La)O for BSLCO and (Sr,Bi)O for pure samples], it is expected that the $c$-axis tunneling matrix element $t_\perp$ is also different; it appears that $t_\perp$ is larger in the pure samples, though the microscopic reason for the difference is not very clear. Second, since the $c$-axis magnetoresistance study of BSLCO has revealed[39] that in the overdoped region the pseudogap is largely due to superconducting fluctuations and thus $T^*$ is governed primarily by $T_c$, the low $T_c$ value of the pure sample is the reason for the low onset temperature of the insulating behavior.[42]

In Fig. 5(b), one notices that residual resistivity of the pure sample is higher than that of the La-doped
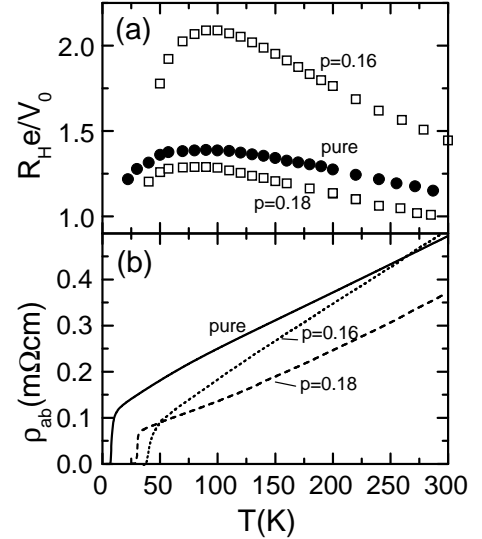
samples, which may be counter-intuitive for a "pure" sample. It is important to recognize, however, that the composition of the "pure" sample is $Bi_{2.13}Sr_{1.89}CuO_{6+\delta}$, which means that there is sizable disorder in the Sr-O block due to excess Bi. (It is known that stoichiometric $Bi_{2.0}Sr_{2.0}CuO_{6+\delta}$ is unstable and cannot be grown.) The larger residual resistivity and the lower $T_c$ of the pure sample suggest that the disorder due to (Sr,Bi) substitution is more harmful to the electronic system in this

material than the disorder due to (Sr,La) substitution.

## B. Two origins of the pseudogap

It is worthwhile to mention that previous measurements of the $c$-axis magnetoresistance of BSLCO have uncovered two additive mechanisms for the pseudogap.[39] In underdoped samples, a magnetic-field-insensitive pseudogap emerges at $T^*$, and a distinct one is formed above $T_c$ as a precursor to superconductivity (which is essentially the superconducting fluctuations); it was found that the latter is mostly responsible for large negative magnetoresistance in $\rho_c$. In overdoped samples, on the other hand, it is only the precursor to superconductivity that appears above $T_c$ and serves as pseudogap.

Recently, scanning tunneling spectroscopy (STS) measurements have been done on our pure samples (which is overdoped) and the pseudogap was found to open below $68\pm2$ K.[43] In Fig. 3(a), the minimum in $\rho_c(T)$ of the pure sample is observed at 70 K, which actually agrees with $T^*$ determined by STS and gives strong support to the interpretation that the steeply insulating behavior in $\rho_c(T)$ is largely due to the suppression of the DOS in BSLCO. Moreover, the STS study has concluded[43] that the pseudogap and the superconductivity has a common origin in our pure sample, which is in agreement with the conclusion drawn from the magnetoresistance study[39] that the pseudogap in the overdoped region is in fact a precursor to superconductivity.

## C. Temperature dependence of $\rho_c$

During the course of the analysis of our $\rho_c(T)$ data, we found that the log-log plot of the data (Fig. 6) uncovers intriguing systematics. In Fig. 6, one can see that for most of the compositions there is a finite range of temperature where the $\rho_c(T)$ data can be roughly described by $T^{-\alpha}$ with $\alpha \simeq 1$ (thin solid lines in Fig. 6). Since the pseudogap is known to cause a rapid increase in $\rho_c$ with decreasing $T$, it is natural to interpret that the observed $T^{-\alpha}$ dependence of $\rho_c$ is caused by the development of the pseudogap; this interpretation motivates us to evaluate the temperature $T_1$ below which the $\rho_c(T)$ obeys the $T^{-\alpha}$ dependence. As shown in Fig. 7, the $p$-dependence of $T_1$, as well as the value of $T_1$ itself, is consistent with what one expects for the pseudogap temperature $T^*$.[6,15,38,39]

An interesting feature in the data in Fig. 6 is that the $\rho_c(T)$ data tend to deviate downwardly from the $T^{-\alpha}$ ($\alpha \simeq 1$) dependence at lower temperatures in underdoped samples; moreover, the characteristic temperature for this deviation, $T_2$, systematically moves to higher temperature with decreasing $p$. In the light of the current understanding of the $c$-axis transport phenomena in cuprates, it is most reasonable to interpret this deviation to come from a saturation of the rapid pseudogap opening, and the more slower increase in $\rho_c$ below $T_2$ is
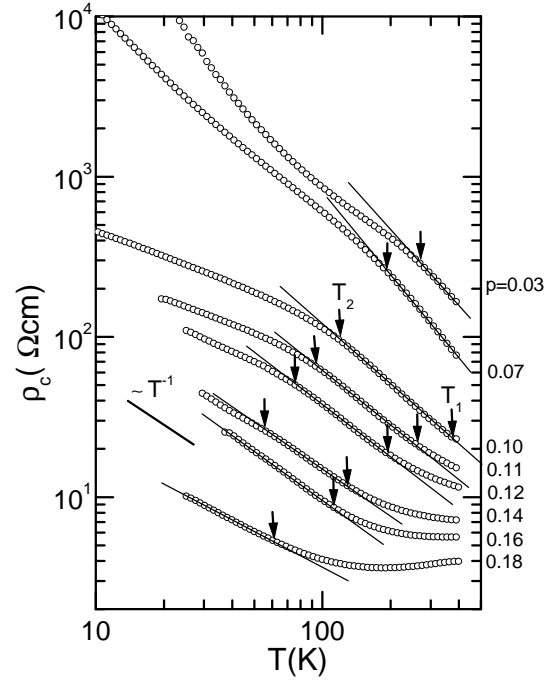


FIG. 6: Double-logarithmic plot of the temperature dependences of $\rho_c$ up to 400 K. Thin solid lines are fits of the intermediate-temperature data to a $T^{-\alpha}$ dependence with $\alpha \simeq 1$. The slope for $\alpha = 1$ is shown in the figure. Arrows mark $T_1$ and $T_2$, between which the $T^{-\alpha}$ dependence is observed.
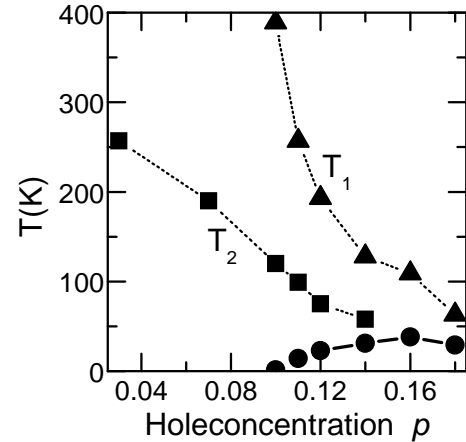


FIG. 7: $T$ vs $p$ diagram to show $T_1$ (our estimate of $T^*$ from the $\rho_c(T)$ data, triangles), $T_2$ (characteristic temperature for the saturation of the pseudogap development, squares), and $T_c$ (circles).

likely to be due to the temperature dependence in the strength of the confinement. Therefore, the temperature dependence of $\rho_c$ as revealed in the log-log plot appears to reflect the fact that the "insulating" behavior is caused by the two phenomena, the pseudogap and the confinement. This is new information which the systematics of our data allows us to infer. (The low-temperature data
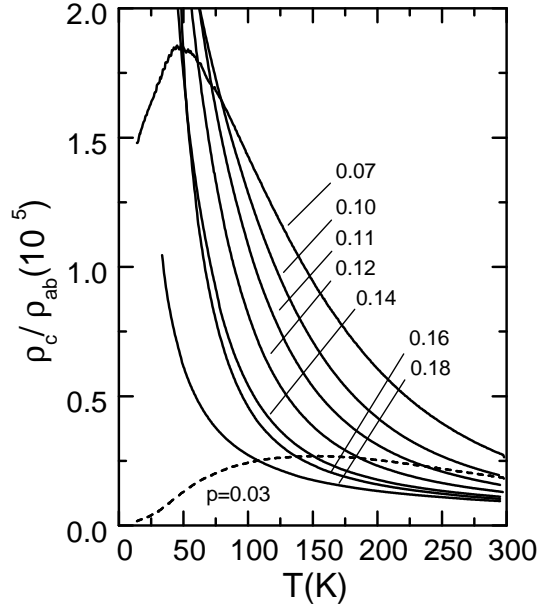
FIG. 8: Temperature dependences of $\rho_c/\rho_{ab}$ of the BSLCO crystals plotted in linear scale.

of the non-superconducting samples ($p = 0.03$ and $0.07$), which show steeper divergence below $T_2$ compared to the superconducting samples, are probably affected by the additional effect of localization.)

We note that the effect of superconducting fluctuations, which cause additional pseudo-gapping near $T_c$,[39] appears to be inconsequential in the overall behavior of the underdoped samples shown in Fig. 6, and the evolution of $T_2$ with $p$ is unrelated to $T_c$. This is probably because the additional reduction in the DOS near $T_c$ due to superconducting fluctuations is relatively small in underdoped samples, which can be inferred by the small size of the magnetoresistance[39] observed in underdoped samples.

It is useful to mention that several empirical temperature dependences have been proposed to describe the $\rho_c(T)$ data of cuprates. In particular, $\rho_c(T) = (a/T)e^{(\Delta/T)} + bT + c$ has been reported to fit the $\rho_c(T)$ data of Bi-2212 very well,[24,44] while $\rho_c(T) = a_0 + aT + 1/(bT + c)$ has been reported to fit the $\rho_c(T)$ data of BSLCO.[25] We have tried to fit our data using these formulae, and found that the latter formula fits well to the data for $p = 0.16$ and $0.18$; however, neither of them fits well to the data for underdoped samples, which is apparently due to the existence of "$T_2$" below which the divergence of $\rho_c(T)$ weakens. Therefore, the extended range of doping of our study unveils the limitation of empirical temperature dependences.
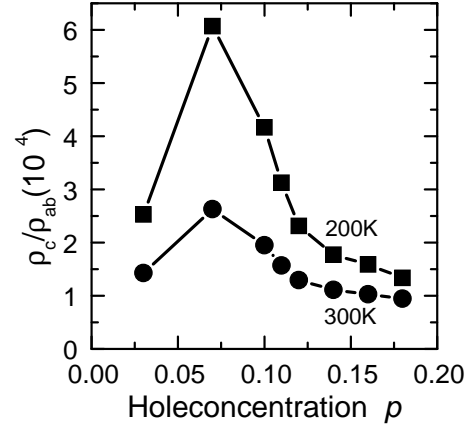


FIG. 9: $p$ dependences of $\rho_c/\rho_{ab}$ at 200 K and 300 K.

**D.** $\rho_c/\rho_{ab}$

Figure 8 replots the $\rho_c/\rho_{ab}$ data of Fig. 4 using a linear scale, which makes it easier to infer the quantitative change of the anisotropy with doping. In Fig. 8, one can see that at high temperatures the $\rho_c/\rho_{ab}$ value drops rapidly with increasing $p$ for $p \geq 0.07$, but this rapid change tends to saturate in highly doped samples ($p \geq 0.14$); this situation can be understood more graphically by plotting the $p$ dependence of $\rho_c/\rho_{ab}$ at 200 K and 300 K, as is shown in Fig. 9. It can be seen in Fig. 9 that at 200 K the $p$ dependence of $\rho_c/\rho_{ab}$ for high doping ($p \geq 0.14$) is weak, while the $\rho_c/\rho_{ab}$ value steeply increases with decreasing $p$ for lower doping ($p \leq 0.12$), except for $p = 0.03$. It is most likely that the weak $p$ dependence at high doping reflects the change in the strength of the charge confinement, while the steep increase in the underdoped samples reflects the enhancement of the anisotropy due to the pseudogap. In fact, the $T_1$ value we determined in Fig. 6 is near 200 K for $p = 0.12$. Therefore, the peculiar hole-doping dependence of the anisotropy is understood to be a combined result of the confinement and the pseudogap.

In Fig. 8, one notices that for non-superconducting concentrations ($p = 0.03$ and $0.07$) there is a peak in the temperature dependence of $\rho_c/\rho_{ab}$ (at 50 and 100 K, respectively), and below the peak temperature the anisotropy is diminished. In particular, $\rho_c/\rho_{ab}$ for $p = 0.03$ decreases dramatically with decreasing $T$, suggesting that the system is heading towards an anisotropic three-dimensional (3D) state for $T \to 0$. Such diminishment of $\rho_c/\rho_{ab}$ has also been observed in insulating samples of Bi-2212 (Ref. 45) and LSCO (Ref. 26), and has been discussed to be due to localization of carriers. In fact, when the carriers are completely localized and becomes immobile in *any* direction, it is natural to see the system as a "3D" insulator; note that the system is expected to retain some amount of anisotropy in the 3D-insulating state, reflecting the anisotropy of the "bare" matrix elements.
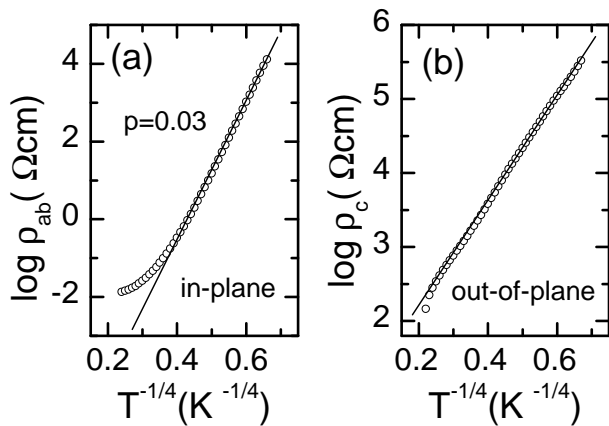
FIG. 10: (a,b) Log of $\rho_{ab}(T)$ and $\rho_c(T)$ of the BSLCO crystals at $p = 0.03$ plotted vs $T^{-1/4}$. The dotted lines are fits of the data to the variable-range hopping dependence $\rho \sim \exp[(T_0/T)^{1/4}]$.

Using the resistivity data for $p = 0.03$, where the superconductivity is lost and carriers are localized due to disorder, we can actually confirm that the system is approaching a 3D insulator. Figure 10 shows the 3D variable range hopping (VRH) plots of $\rho_{ab}(T)$ and $\rho_c(T)$ for $p = 0.03$. The dotted lines are fits to the expected temperature dependence for the 3D VRH, $\rho \sim \exp[(T_0/T)^{1/4}]$. Since the 3D-VRH formula describes the temperature dependences of both $\rho_{ab}$ and $\rho_c$ very well, one can conclude that the charge transport along *all* directions is governed by the *same* mechanism, giving a rationale to call the system to be an anisotropic 3D insulator. The fits give $T_0$ values of $2.6 \times 10^6$ K and $8.6 \times 10^4$ K for $\rho_{ab}(T)$ and $\rho_c(T)$, respectively. These values are in the same range as the $T_0$ values obtained for flux-grown LSCO crystals in the lightly-doped regime,[46] but the source of its anisotropy

is not clear at this stage.

## V. SUMMARY

Systematic measurements of the $c$-axis resistivity $\rho_c$ and the resistivity anisotropy ratio $\rho_c/\rho_{ab}$ of BSLCO for a wide doping range showcase that the anisotropy is determined by three mechanisms: charge confinement, pseudogap, and localization. At high temperature and in highly doped samples, the charge confinement is the sole determining factor, and thus one can measure the intrinsic strength of the charge confinement in this corner of the phase diagram; our data indicate that without the effect of the pseudogap the $\rho_c/\rho_{ab}$ value is order of $10^4$ for BSLCO. At low temperature and in low doped samples, the localization governs the charge transport and the $\rho_c/\rho_{ab}$ ratio is diminished. In underdoped superconducting samples, the pseudogap significantly enhances the $\rho_c/\rho_{ab}$ value with decreasing temperature, causing $\rho_c/\rho_{ab}$ to reach $\sim 10^6$. Close examination of the temperature dependence of $\rho_c$ of underdoped samples finds that below $T^*$ there are two distinct temperature regions where the divergence of $\rho_c$ appears to be governed by different mechanisms; the data suggest that the development of the pseudogap leads to a $T^{-\alpha}$ dependence of $\rho_c$ with $\alpha \simeq 1$ below $T^*$, while at lower temperature $\rho_c$ shows a weaker temperature dependence where we argue that the charge confinement dictates the $T$ dependence. Since the effect of the pseudogap is apparently lacking in the anisotropic behavior of LSCO,[26] the BSLCO system offers a complementary testing ground to study the source of the peculiar $c$-axis transport in the cuprate superconductors.

[*] ando@criepi.denken.or.jp

[1] For a review, see S. L. Cooper and K. E. Gray, in *Physical Properties of High Temperature Superconductors IV*, edited by D. M. Ginsberg (World Scientific, Singapore, 1994).

[2] P. W. Anderson, Science **256**, 1526 (1992).

[3] W. E. Pickett, Rev. Mod. Phys. **61**, 433 (1989).

[4] S. Martin, A. T. Fiory, R. M. Fleming, L. F. Schneemeyer, and J. V. Waszczak, **60**, 2194 (1988).

[5] Y. Nakamura and S. Uchida, Phys. Rev. B **47**, 8369 (1993).

[6] K. Takenaka, K. Mizuhashi, H. Takagi, and S. Uchida, Phys. Rev. B **50**, 6534 (1994).

[7] Y. Ando, G. S. Boebinger, A. Passner, N. L. Wang, C. Geibel, and F. Steglich, Phys. Rev. Lett. **77**, 2065 (1996).

[8] P. W. Anderson and Z. Zou, Phys. Rev. Lett. **60**, 132 (1988).

[9] N. Nagaosa, Phys. Rev. B **52**, 10561 (1995).

[10] E. W. Carlson, D. Orgad, S. A. Kivelson, and V. J. Emery, Phys. Rev. B **62**, 3422 (2000).

[11] J. Zaanen, Science **286**, 251 (1999).

[12] L. B. Ioffe and A. J. Millis, Phys. Rev. B **58**, 11631 (1998).

[13] R. Kleiner and P. Müller, Phys. Rev. B **49**, 1327 (1994).

[14] M. Tachiki, T. Koyama, and S. Takahashi, Phys. Rev. B **50**, 7065 (1994).

[15] T. Timusk and B. Statt, Rep. Prog. Phys. **62**, 61 (1999).

[16] M. R. Norman, H. Ding, M. Randeria, J. C. Campuzano, T. Yokoya, T. Takeuchi, T. Takahashi, T. Mochiku, K. Kadowaki, P. Guptasarma, and D. G. Hinks, Nature (London) **392**, 157 (1998).

[17] T. Xiang and J. M. Wheatley, Phys. Rev. Lett. **77**, 4632 (1996),

[18] M. Suzuki and T. Watanabe, Phys. Rev. Lett. **85**, 4787 (1999).

[19] V. M. Krasnov, A. Yurgens, D. Winkler, P. Delsing, and T. Claeson, Phys. Rev. Lett. **84**, 5860 (2000).

[20] T. Kimura, K. Kishio, T. Kobayashi, Y. Nakayama, N. Motohira, K. Kitazawa, and K. Yamafuji, Physica C **192**, 247 (1992).

[21] Y. Ando, G. S. Boebinger, A. Passner, T. Kimura, and K. Kishio, Phys. Rev. Lett. **75**, 4662 (1995).

[22] G. S. Boebinger, Y. Ando, A. Passner, T. Kimura, M.

Okuya, J. Shimoyama, K. Kishio, K. Tamasaku, N. Ichikawa, and S. Uchida, Phys. Rev. Lett. **77**, 5417 (1996).

[23] I. Terasaki, Y. Sato, S. Miyamoto, S. Tajima, and S. Tanaka, Phys. Rev. B **52**, 16246 (1995).

[24] T. Watanabe, T. Fujii, and A. Matsuda, Phys. Rev. Lett. **79**, 2113 (1997).

[25] N. L. Wang, B. Buschinger, C. Geibel, and F. Steglich, Phys. Rev. B **54**, 7449 (1996).

[26] S. Komiya, Y. Ando, X. F. Sun, and A. N. Lavrov, to appear in Phys. Rev. B (cond-mat/0203107).

[27] X. J. Zhou, P. V. Bogdanov, S. A. Kellar, T. Noda, H. Eisaki, S. Uchida, Z. Hussain, and Z.-X. Shen, Science **286**, 268 (1999).

[28] A. Ino, C. Kim, M. Nakamura, T. Yoshida, T. Mizokawa, Z.-X. Shen, A. Fujimori, T. Kakeshita, H. Eisaki, and S. Uchida, Phys. Rev. B **62**, 4137 (2000).

[29] Y. Ando and T. Murayama, Phys. Rev. B **60**, R6991 (1999).

[30] S. Ono, Y. Ando, T. Murayama, F. F. Balakirev, J. B. Betts, and G. S. Boebinger, Phys Rev. Lett. **85**, 638 (2000).

[31] Y. Ando, Y. Hanaki, S. Ono, T. Murayama, K. Segawa, N. Miyamoto, and S. Komiya, Phys. Rev. B **61**, R14956 (2000); **63**, 069902(E) (2001).

[32] J. M. Harris, P. J. White, Z. -X. Shen, H. Ikeda, R. Yoshizaki, H. Eisaki, S. Uchida, W. D. Si, J. W. Xiong, Z. -X. Zhao, and D. S. Dessau, Phys. Rev. Lett. **79**, 143 (1997).

[33] Y.-D. Chuang, A. D. Gromko, D. S. Dessau, Y. Aiura, Y. Yamaguchi, K. Oka, A. J. Arko, J. Joyce, H. Eisaki, S.I. Uchida, K. Nakamura, and Y. Ando, Phys. Rev. Lett. **83**, 3717 (1999).

[34] T. Sato, T. Kamiyama, T. Takahashi, J. Mesot, A. Kaminski, J. C. Campuzano, H. M. Fretwell, T. Takeuchi, H. Ding, I. Chong, T. Terashima, and M. Takano, Phys. Rev.

B **64**, 054502 (2001).

[35] A. P. Mackenzie, S. D. Hughes, J. R. Cooper, A. Carrington, C. Chen, and B. M. Wanklyn, Phys. Rev. B **45**, 527 (1992).

[36] Y. Ando, A. N. Lavrov, Seiki Komiya, Kouji Segawa, and X. F. Sun, Phys. Rev. Lett. **87**, 017001 (2001).

[37] Y. Fukuzumi, K. Mizuhashi, K. Takenaka, and S. Uchida, Phys. Rev. Lett. **76**, 684 (1996), and references therein.

[38] T. Watanabe, T. Fujii, and A. Matsuda, Phys. Rev. Lett. **84**, 5848 (2000).

[39] A. N. Lavrov, Y. Ando, and S. Ono, Europhys. Lett. **57**, 267 (2002).

[40] N. Kumar and A. M. Jayannavar, Phys. Rev. B **45**, 5001 (1992).

[41] N. E. Hussey, J. R. Cooper, Y. Kodama, and Y. Nishihara, Phys. Rev. B **58**, R611 (1998).

[42] The BSLCO samples used in Ref. 39 were taken from the same batch as the samples used in the present study, but they were annealed with different conditions; this caused the $T_c$ values for the same composition to be lower in the samples of Ref. 39. This difference in $T_c$ (which affects $T^*$ in the overdoped region) is the reason for apparently different behaviors of $\rho_c(T)$ between the two studies.

[43] M. Kugler, O. Fischer, Ch. Renner, S. Ono, and Y. Ando, Phys. Rev. Lett. **86**, 4911 (2001).

[44] Y. F. Yan, P. Matl, J. M. Harris, and N. P. Ong, Phys. Rev. B **52**, R751 (1995).

[45] T. Kitajima, T. Takayanagi, T. Takemura, I. Terasaki, J. Phys. Condens. Matter **11**, 3169 (1999).

[46] C. Y. Chen, E. C. Branlund, C.S. Bae, K. Yang, M. A. Kastner, A. Cassanho, and R. J. Birgeneau, Phys. Rev. B **51**, 3671 (1995).